Desalination and Water Treatment
www.deswater.com
doi: 10.1080/19443994.2015.1019371

57 (2016) 8194–8203
April

Taylor & Francis
Taylor & Francis Group

Size fractionation of elements and nanoparticles in natural water by both dead-end and tangential flow filtration

N. Wu[a,1], Y. Wyart[a], J. Rose[b,c], B. Angeletti[d], P. Moulin[a,*]

[a]*Aix Marseille Université, CNRS, Centrale Marseille, M2P2 UMR 7340, Equipe Procédés Membranaires (EPM), Europôle de l'Arbois, BP80, Pavillon Laennec, Hall C, 13545 Aix-en-Provence Cedex 4, France, Tel. +33 4 42 90 85 01; emails: nwu@tjau.edu.cn (N. Wu), yvan.wyart@univ-amu.fr (Y. Wyart), Tel. +33 4 42 90 85 01; Fax: +33 4 42 90 85 15; email: philippe.moulin@univ-amu.fr (P. Moulin)*
[b]*CNRS, CEREGE, UMR 7330, (FR ECCOREV), 13545 Aix-en-Provence Cedex 4, France, Tel. +33 4 42 97 15 29; email: rose@cerege.fr*
[c]*CNRS, Duke University, International Consortium for the Environmental Implications of Nanotechnology iCEINT, Europôle de l'Arbois, 13545 Aix-en-Provence Cedex 4, France*
[d]*Aix Marseille Université, CEREGE, UMR 7330, 13545 Aix-en-Provence Cedex 4, France, Tel. +33 4 42 97 15 12; email: angeletti@cerege.fr*

Received 22 September 2014; Accepted 6 February 2015

ABSTRACT

The influence of membrane filtration modes on the estimation of size distribution for natural elements in water was investigated. The stepwise membrane filtration is used to distinguish different size fractions including large particulate (>18 μm), particulate (0.2–18 μm), colloidal/nanoparticle (10 kDa–0.2 μm), and truly dissolved fractions (<10 kDa) in river water samples and wastewater treatment plants effluents. Dead-end and tangential flow filtrations were compared during fractionation process. For most elements, concentrations in different size fractions obtained by two filtration modes were generally similar. The obvious difference was only found in acid fractions for some elements, which might be related to the cake grown at membrane surfaces between two filtration modes. In case of elemental partitioning, the influence of filtration modes was normally negligible, when the membranes used and operational factors were exactly the same.

Keywords: Colloids; Nanoparticles; Membrane; Filtration mode; Surface water

1. Introduction

With the rapid development of semiconductor and nanotechnology industries, some elements used in these industries could be released into receiving waters via sewage effluents [1,2]. However, knowledge of the concentrations of these elements in receiving waters is substantially lacking [2,3], especially for the elements associated with colloidal/nanoparticle fractions or even used under nanoparticulate form. Due to the complexity and polydispersity of aquatic colloids/nanoparticles, the sample fractionation is often required prior to analysis [4]. Membrane

*Corresponding author.

[1]Present address: College of Engineering and Technology, Tianjin Agricultural University, 300384 Tianjin, China, Tel. +86 22 23781291.

filtration is one of the most commonly used size fractionation techniques [5].

Size fractionation of natural water by membrane filtration can be carried out through dead-end filtration (DEF) or tangential flow filtration (TFF). But it is still unclear which kind of filtration mode can achieve a better size fractionation, particularly for the part of aquatic nanomaterials/colloids. On one hand, some studies selected DEF to assess the colloidal forms of trace elements in river water or estuaries [6–8]. Guéguen et al. [9] recommended the DEF for its easy handling, since TFF possibly required large-volume samples (i.e. 10–1,000 L) and was relatively time consuming depending on the desired concentration factor. Also, it is doubtful that TFF could be used at significantly higher flow rates than DEF without gel formation above the membrane surface leading to errors in the size discrimination [10]. On the other hand, a number of studies employed TFF instead of DEF to collect and separate nanomaterials/colloids, since TFF is likely to reduce some fouling problems like concentration polarization and clogging caused by DEF [3,11–13].

In this paper, the industrial zone (IZ) of Rousset–Peynier (Provence, France), known as "Silicon Valley of Provence" was selected because a large number of companies in the field of microelectronics, nanotechnology, and surface treatment of components (wafer polishing) are located there. In this area, industrial effluents are treated by a specific wastewater treatment plants (WWTPs) of the IZ after recycling and treatment at each site, before they are discharged into the Arc River [14]. Surface water samples from upstream, WWTP effluents of the IZ, and downstream of the Arc River were analyzed. Filter cartridges (18 μm) and membranes with decreasing pore size/MWCO (0.2 μm and 10 kDa) were used to distinguish large particulate (i.e. >18 μm), particulate (i.e. 0.2–18 μm), colloidal/nanoparticle (i.e. 10 kDa–0.2 μm), and truly dissolved fractions (i.e. <10 kDa). After a similar pre-filtration (18 μm), both DEF and TFF modes were tested on the same water sample, in order to investigate the effects of filtration modes on the estimation of size distribution for elements in water samples. The size distribution is given by the membrane molecular weight cutoff (MWCO) given by the manufacturers.

2. Materials and methods

2.1. Sampling sites

Water samples were collected from the IZ of Rousset–Peynier in France (September 2012). As depicted in our previous work [14], the WWTP effluent of IZ, defined as "Outlet," was collected right before its release into the Arc River, and the other two surface water samples were taken from the upstream and downstream of the Arc River. About 20 L water samples (10 L for each filtration mode) were collected for each site. Samples were collected in plastic bottles that had been washed with 0.1 M super-pure HNO_3 and rinsed with Milli-Q water. Within 1–2 h of sampling, raw water samples were transported to the laboratory and immediately processed for analysis (i.e. pH and conductivity) and pre-filtration.

2.2. Fractionation processes

The schematic layout of the sample preparation protocol is given in Fig. 1. Raw water was firstly filtered by Rigimesh® sintered metal mesh filter cartridges (MBS1001RK, PALL) with a pore size of 18 μm in order to remove large particles. The outlet from the cartridge was collected as feed water. Then, a two-step filtration was immediately undertaken using 0.2 μm polyvinylidene fluoride hollow fiber membrane (UMP-0047R, Microza, PALL) and 10 kDa polyethersulfone cassette membrane (Sius-LS TFF, HyStream, LP screen channel, Novasep). The clean membranes permeabilities ($T = 20$°C) were 922 ± 128 and 157 ± 8 L h^{-1} m^{-2} bar^{-1} for the 0.2 μm and 10 kDa membranes, respectively.

A two-step filtration was carried out for feed water. Two different filtration methods were used in this study: TFF and DEF, which were all performed using the AutoPurification System (PureTec™, Scilog-Inc, USA), as presented in Fig. 2. The PureTec™ system is a software-driven fluid delivery system that automatically monitors and adjusts transmembrane pressure (TMP) or cross flow rate, and records filtration parameters over time. The system is mainly composed of peristaltic pump, feed tank, stirrer, balance, membrane filter, permeate reservoir, three pressure

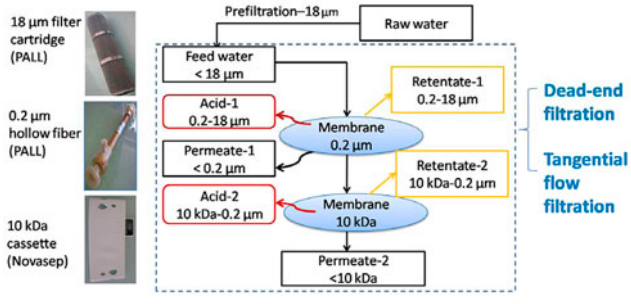

Fig. 1. Schematic layout of the sample preparation protocol.

sensors (P1, P2, and P3), conductivity monitor with conductivity/temperature sensor, and SciDoc data collection software. The additional tank is used to increase the capacity of feed tank (10 L).

Prior to filtration experiments, the membranes were thoroughly rinsed by distilled water to remove preservatives by TFF mode until the conductivity of permeate is close to that of distilled water. During the process, only valve 6 was closed. This stage lasted about 30–60 min. The constant pressure mode of PureTec™ system was chosen to enable filtration of samples. TMP was maintained at a constant level for each filtration run (0.6–1.3 bar for 0.2 μm filtrations and 2.5–2.9 bar for 10 kDa filtrations). Filtrate flux was calculated. During the filtration processes, valves 1, 2, and 5 were open, valve 6 was closed. DEF was carried out by closing valve 4. By opening this valve, TFF process can be performed. Valve 3 was partially closed, which is used to increase the pressure of P2 and to achieve a high TMP easily during TFF process. The volume concentration factors ranged from 26 to 28 for 0.2 μm filtrations and from 22 to 25 for 10 kDa filtrations.

At the end of each filtration run (after the collection of permeates and retentates), about 200 mL 0.01 M super-pure HNO_3 solution (pH 2) was flushed through the filtration system, in order to recover as much as possible elements that may have adsorbed to the membrane during filtration. During the process, valves 2, 3, 4, and 6 were opened, valves 1 and 5 were closed. This stage lasted about 30 min, under the TMP of 2 bar. The acid rinsing solutions (define as Acid 1 and 2) were also collected after each membrane filtration step (0.2 μm and 10 kDa) for mass balance analyses. The mass balance for each filtration process and the percentage of each pore size/MWCO fraction for elements were calculated [14].

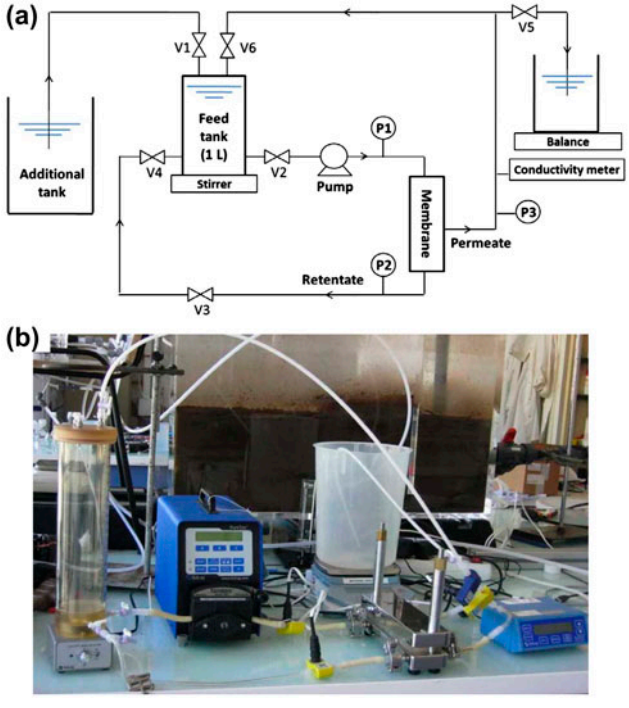

Fig. 2. Pilot-scale filtration system (a) schematic diagram and (b) photo.

2.3. Sample analysis

Water samples for element analyses were stored at 4°C after acidification (pH 1 or 2) with super-pure HNO_3 (15 M). All the samples were analyzed without dilution. Element concentrations were mainly determined by inductively coupled plasma mass spectrometry (ICP-MS, NexION 300X, PerkinElmer). Indium was used as internal standards. Accuracy and precision of ICP-MS measurements were checked using certified reference materials SLRS-4 (fresh water sample) from the National Research Council of Canada, which were within 5% of the certified values for the elements of interest. The detection limits for elements generally ranged from 0.01 to 1 $\mu g\,L^{-1}$, except for Si (19.61 $\mu g\,L^{-1}$) and Fe (3.30 $\mu g\,L^{-1}$).

The pH of samples was measured with a microprocessor pH meter (HANNA, pH210), and the conductivity was measured using WTW Cond 3310 Handheld Conductivity Meters (Germany). Turbidity of raw water was analyzed by WTW Turb 550 IR turbidity meter. UV absorption at 254 nm (UV_{254}) of raw water was measured by JENWAY 6715 UV/Vis spectrophotometer. Total organic carbon (TOC) was determined using a Shimadzu TOC-VCPH analyzer. The detection limit was 4 $\mu g\,L^{-1}$. The particle size distribution of samples (i.e. feed, retentate 1) was evaluated by Malvern Mastersizer 3000 laser diffraction particle size analyzer.

3. Results and discussion

3.1. Characteristics of raw water

The main chemical parameters for raw water of different sites are presented in Table 1. The pH values of raw water for the three sampling sites were near neutral and rather similar, ranging from 7.60 to 7.77. The conductivity values of raw water from river (upstream and downstream) were relatively constant, ranging from 1,509 to 1,530 $\mu S\,cm^{-1}$ between upstream and downstream, but were much higher than that (945 $\mu S\,cm^{-1}$) measured in WWTP effluent (outlet).

Table 1
Main chemical parameters for raw water in three sampling sites (element concentrations are represented by "mean ± standard deviation")

	Upstream	Outlet	Downstream	Detection limits
pH	7.77	7.60	7.65	–
Conductivity ($\mu S\,cm^{-1}$)	1,509	945	1,530	–
Turbidity (NTU)	4.6	8.0	6.2	–
UV_{254} (cm^{-1})	0.056	0.161	0.067	–
TOC ($mg\,L^{-1}$)	2.81	5.80	2.96	0.004
Si ($\mu g\,L^{-1}$)	3,623.04 ± 30.87	2,924.08 ± 29.77	3,583.19 ± 16.33	19.61*
Fe ($\mu g\,L^{-1}$)	50.23 ± 1.39	85.68 ± 1.81	84.02 ± 1.12	3.30*
Co ($\mu g\,L^{-1}$)	0.117 ± 0.007	0.412 ± 0.009	0.192 ± 0.006	0.004*
Cu ($\mu g\,L^{-1}$)	8.963 ± 0.066	7.621 ± 0.098	10.319 ± 0.114	0.028*
As ($\mu g\,L^{-1}$)	0.513 ± 0.031	0.274 ± 0.033	0.543 ± 0.026	0.015*
Sc ($\mu g\,L^{-1}$)	0.042 ± 0.014	0.028 ± 0.002	0.033 ± 0.008	0.025*
Sr ($\mu g\,L^{-1}$)	481.94 ± 6.08	350.12 ± 2.30	485.41 ± 4.96	0.004*
Cd ($\mu g\,L^{-1}$)	12.742 ± 0.185	0.827 ± 0.014	0.080 ± 0.019	0.002*
Sb ($\mu g\,L^{-1}$)	0.230 ± 0.020	0.584 ± 0.042	0.294 ± 0.005	0.005*
Cs ($\mu g\,L^{-1}$)	0.062 ± 0.004	0.047 ± 0.000	0.067 ± 0.001	0.023*
Gd ($\mu g\,L^{-1}$)	0.043 ± 0.002	0.467 ± 0.001	0.065 ± 0.003	0.020*

*Detection limits of ICP-MS were calculated as three times the standard deviations of analytical blanks.
–Not determined.

Contrary to the conductivity, the maximum values of turbidity and UV_{254} were observed at the outlet. It can be seen that TOC contents at the outlet were higher than those in river water, which are in good agreement with the tendency obtained in UV_{254} analysis. The higher contents of TOC at the outlet may be related to the flocculants used in WWTPs.

Total concentrations of elements in raw water for three sampling sites are also given. In general, the concentrations of major elements measured in river water were below accepted concentrations for drinking water [15], except for Cd. The higher concentration of Cd (2.5 times than drinking water standards) was only observed upstream. This occurrence was not associated with IZ contribution, since the water withdrawals from the river were performed upstream of the WWTP outlet and also Cd concentration was low at the WWTP outlet.

For elements Fe, Co, Cu, Sb, and Gd, their total concentrations downstream increased, compared to upstream. On one hand, for Co, Sb, and Gd, their concentrations at the WWTP outlet were higher than in river water. Thus, the increase in concentrations of Co, Sb, and Gd downstream could be caused by a discharge of these elements via WWTP effluent into river water, although it cannot be concluded that effluent was the only contributor. On the other hand, for other elements like Cu, their concentrations at the WWTP outlet were lower than or similar to those in river water. Thus, the increase in their concentrations downstream could be attributed to other factors (i.e. geochemical behaviors of elements, or other unknown sources) rather than the inputs of WWTP effluent. In the particular case of Fe (used as coagulant), its concentration at the WWTP is high and remains high downstream. This may be due to the WWTP contribution.

3.2. Size distribution in feed and retentate

Fig. 3 describes the particle size distribution of feed (<18 μm) and retentate 1 (0.2–18 μm) from three sampling sites. The size distribution for lower fractions was not studied. For feed water, the values of Dv 90 (particle size below which 90% of the volume of particles exists) upstream and downstream were 27 and 22.3 μm, respectively. The results indicated that the 18 μm prefiltration could generally realize a desirable separation of large particles from water. But there still exist some larger particles than 18 μm (the pore size of the mesh filter cartridge) in filtered samples. This phenomenon might be caused by very rapid aggregation of some small particles in filtered water during the period of about 30 min (samples were transported to the place for size analysis after the filtration end). Moreover, the Dv 90 value of 105 μm in the WWTP outlet-feed water was about 4–5 times higher than feed water from upstream and downstream. This difference can be due to the own characteristics of samples and the influence of the WWTP. It also can be due to some problem during the settling phase of the WWTP operations.

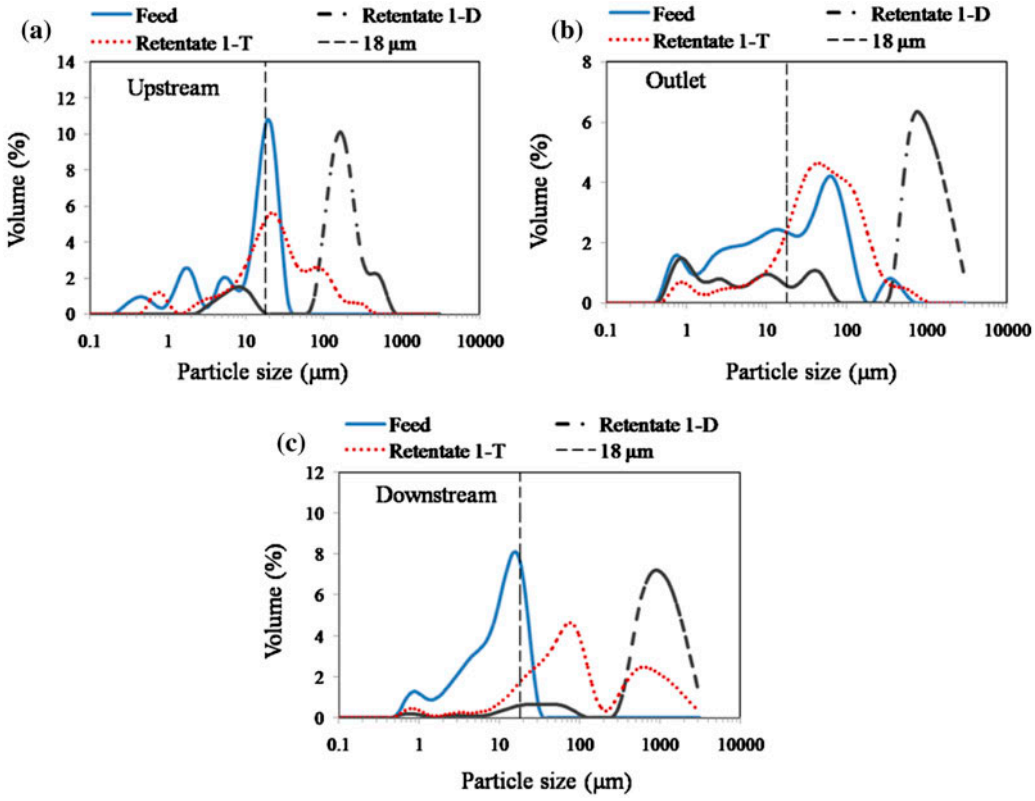

Fig. 3. Particle size distribution of feed (<18 μm) and retentate 1 (0.2–18 μm) from (a) upstream, (b) outlet, and (c) downstream (D: DEF; T: TFF). Size distributions were measured by Malvern Mastersizer 3000 laser diffraction particle size analyzer.

Compared to feed water, the increase of sizes in retentate 1 could be explained by particle aggregations during filtration processes and/or aggregation during sample storage (even the storage duration was short). With regards to the influence of filtration modes on size distributions, the results showed that the sizes of retentate 1 (0.2–18 μm) by DEF were obviously larger than those by TFF for all three sampling sites. This suggested that DEF resulted in aggregation of particles (0.2–18 μm) to a larger degree, compared to TFF. The reason for the larger aggregates formation could be related to the greater level of fouling during DEF than TFF.

3.3. Mass balance recoveries

Fig. 4 depicts the mass balance recoveries (%) measured for each filtration process (0.2 μm and 10 kDa) obtained by DEF and TFF. The recovery efficiencies of TOC for all three sampling sites by both filtration modes were satisfying, within the range from 89 to 104%. The recoveries of elements Si, Co, As, Sr, Cd, Sb, Cs, and Gd were within the range of 70–130%, in both 0.2 μm and 10 kDa filtration by two filtration modes for all sampling sites. According to Babiarz et al. [16], the mass balance within ±30% is considered reasonable for data validation. For these elements, the mass balance values obtained by two filtration modes (DEF and TFF) were generally similar.

For elements Fe, Cu, and Se, their mass balance recoveries were not always acceptable. For Fe, low recoveries (52–61%) were observed during 0.2 μm filtration of downstream water regardless of the filtration modes. This result was consistent with our previous studies (37% recovery for Fe during 0.2 μm filtration of upstream water) [14]. Other authors also reported the low recoveries of Fe in river water (71%) [17], seawater (47–60%) [18], and sediment pore water (71%) [19]. This phenomenon could be attributed to the trapping of Fe-compounds inside membranes or sorption to the membranes. Incomplete recoveries were also observed for Cu downstream during 0.2 μm and 10 kDa filtration and for Se in 10 kDa-TFF upstream. But for Cu and Se, their recoveries in some parts were over 130%, possibly due to the analytical uncertainty and/or contamination. Similarly, the mass balance of Cu in sediment pore water was found to be 150% and highly variable [19].

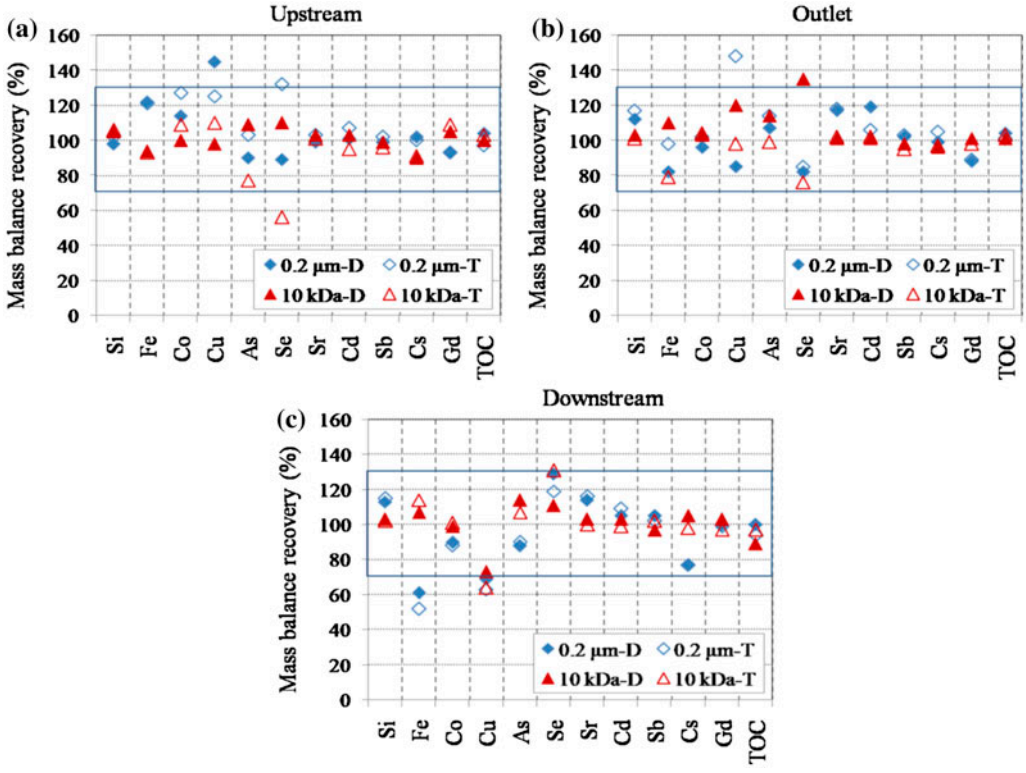

Fig. 4. Mass balance recovery (%) of elements for three sampling sites by two filtration modes (D: DEF; T: TFF).

3.4. Element concentrations in different fractions by two filtration modes

In order to investigate the influence of filtration modes on the elements partitioning, element concentrations in different fractions obtained by DEF and TFF are compared, as shown in Fig. 5. As described in Section 2.2, the raw water was firstly filtered by 18 µm filter cartridges to get the outlet as feed water. Then the feed water was divided into two parts for DEF and TFF (noted D and T, respectively) during the next stepwise filtration 0.2 µm and 10 kDa (noted 1 and 2, respectively). For example, during DEF, feed water was filtered to get permeate 1-D, and then permeate 1-D was filtered to get permeate and retentate 2-D. The same case was with TFF process. Since raw water and feed water for two filtration modes were the same, only the size fractions including permeate 1, retentate 1, acid 1, permeate 2, retentate 2, and acid 2 are compared.

For most elements, the concentrations obtained by two filtration modes were generally similar in different size fractions (i.e. permeates) (Fig. 5). The significant difference was mainly found in acid fractions for some elements, i.e. Si. This observation corresponds to the findings of Dupré et al. [20], who compared the element contents in the 0.20 µm dead-end and tangential filtrates, and found that element concentrations were generally similar except for some elements, such as Al, Mn, Cu, etc. However, they only compared 0.20 µm permeates without studying other size fractions.

In terms of particulate fractions (0.2–18 µm) which include acid 1 and retentate 1, the difference was related to element types and sampling sites. For Si and Sr, their concentrations in acid 1-D were 1.7–1.8 times higher than in acid 1-T for river water, but not for WWTP outlet water. As mentioned previously, the acids were used to flush through the filtration system at the end of filtration run, in order to recover as much as possible elements adsorbed to membranes. Thus, the result indicates that more Si and Sr within particulate fractions (0.2–18 µm) were normally adsorbed and/or retained by the membranes during 0.2 µm DEF, compared with TFF processes. The same case was with Fe (see acid 1 in downstream), but the opposite case was found for Co (see acid 1 in upstream).

With regards to colloidal/nanoparticle fractions (10 kDa–0.2 µm), elements also showed very different behaviors, partly dependent of sampling sites. For elements Fe, Cu, and Sr in river water, their concentrations in acid 2-D were higher (1.5–3.1 times) than in acid 2-T. But the opposite case was observed for Si, whose concentrations in acid 2-T were higher

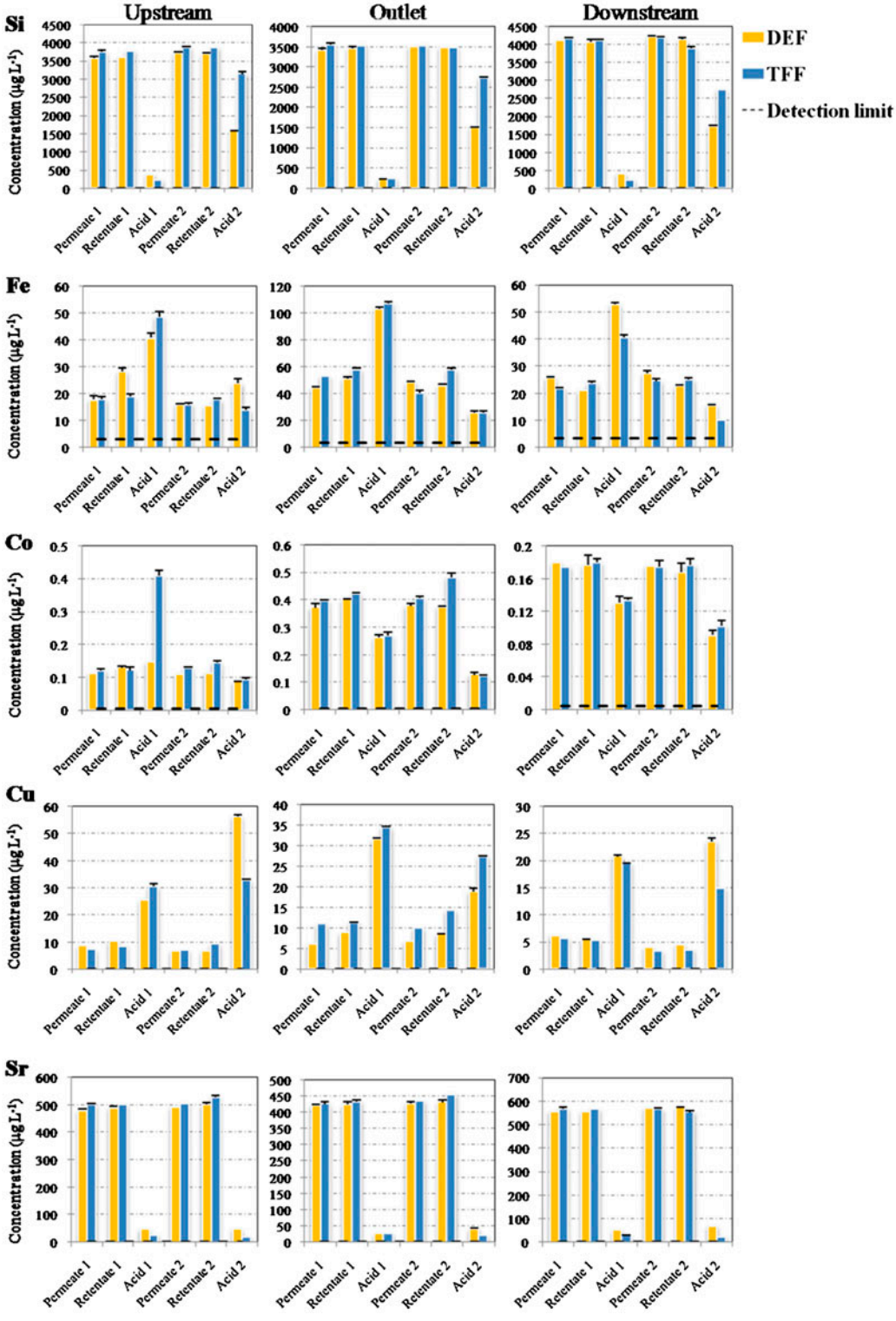

Fig. 5. Concentrations of elements Si, Fe, Co, Cu, and Sr associated with different fractions. Error bars refer to the standard deviations on the average of three repeated measurements.

(1.6–2 times) than in acid 2-D, regardless of sampling sites. Similarly, higher concentrations were found for Co within retentate 2-T in upstream and outlet.

In agreement with the elements (Si, Fe, Co, Cu, and Sr) discussed before, the contents of Cd, As, Sb, Se, Cs, and Gd in different size fractions obtained by two filtration modes were generally similar (data not given), taking into account the analytical uncertainties and detection limits (concentrations in some fractions were close to the detection limits). Overall, the influence of filtration modes on elemental concentrations within size fractions was highly variable, which was dependent on many factors such as element types, water bodies, and the size fractions studied. In conclusion, for many elements, the significant difference for element concentrations was only found in acid fractions between two filtration modes.

3.5. Partitioning of elements by two filtration modes

The percentages of elements in large particulate (>18 μm), particulate (0.2–18 μm), colloidal/nanoparticle (10 kDa–0.2 μm), and truly dissolved (<10 kDa) fractions, which were obtained by DEF and TFF processes are presented in Fig. 6. For this calculation, both data of concentrations and mass balance were used. It should be noted that for large particulate fractions (>18 μm), their separation was performed using the same 18 μm dead-end pre-filtration system. So, there was no difference between D and T for large particulate fractions.

Whatever the sampling sites or the filtration modes, organic matters (TOC indicator) primarily existed as truly dissolved fractions (76–90%). This corresponds to the previous investigation that most of TOC in river water was composed of organic compounds smaller than 0.05 μm [21]. In all samples, elements Si, Co, As, Se, Sr, Cd, Sb, and Cs were mainly found in truly dissolved fractions (72–94%), which showed similar profiles as TOC. The results were in agreement with Casiot et al. [22], who reported that As, Cd, and Co were mainly present in dissolved phases in river waters. For Fe, a considerable part was also found in large particulate fractions (34–69%). This result was consistent with our previous studies [14] and one research on river waters [23]. For Gd in upstream (U-D and U-T), it was almost equally bound to large particulate (42%) and truly dissolved (53%) fractions. For most elements, either the particulate fractions or the colloidal/nanoparticle fractions only occupied a very small part (<10%), except for Cu. For example, the colloidal/nanoparticle fractions of Cu ranged from 9 to 15% among sampling sites, which were slightly higher than those of other elements.

From upstream to downstream, most elements were, more or less, increasingly accumulated in truly dissolved fractions, except for Si and Sr (remained constant). Compared to upstream, the total percentages of particulate and colloidal/nanoparticle fractions for most elements decreased or relatively remained constant in the downstream, except for Cu, Cd, and Gd (increased slightly by 2–4%). However, it could be interesting to discuss the term "truly" dissolved fraction based on 10 kDa filtration. The case of iron is emblematic, since the solubility of iron minerals is quite low at circumneutral pH. Indeed, the solubility of one of the most soluble iron oxyhydroxide phase (ferrihydrite) from Yu et al. [24] is estimated to be $\log K = 8.46 \pm 1.40$ (for 2-line ferrihydrite), based on the following equation for the ferrihydrite dissolution: $Fe_2O_{3-0.5y}(OH)_y + 6H^+ \Rightarrow 2Fe^{3+} + (3 + 0.5y)\ H_2O$. Then the Fe^{3+} concentration at pH 7.7 would be 3.17×10^{-19} mol L^{-1}. However, the Fe concentration range is from 3 to 4×10^{-7} mol L^{-1} for the <10 kDa fraction in all studied waters. This clearly indicates that the filtration at 10 kDa may not be powerful enough to isolate the "truly dissolved fraction." Even the equation relating the size porosity to the MWCO, only provide rough estimation, a 10 kDa membrane might possess pore diameter in a 2–4 nm range, i.e. [25]. Therefore, in the case of iron, for instance, this clearly indicates that Fe is mainly present under the form of Fe-molecule (either Fe–Fe polymers or Fe-organic complexes) and not under the ionic form.

About the influence of filtration modes (D and T) on elemental partitioning, for particulate (0.2–18 μm) fractions, there was almost no variation between two filtration modes for most elements, except for Co, Cu, and Se (slight variation between D and T, ranging from 2 to 4%). For Co and Cu in upstream (U-D and U-T), TFF yielded a slightly higher particulate fraction than DEF; but the opposite case was found for Cu in the WWTP outlet water (O-D and O-T). However, for these 2 cases, the variations were very small. With regard to colloidal/nanoparticle (10 kDa–0.2 μm) fractions, TFF yielded a slightly higher proportion than DEF for elements Si, Fe, As, Se, Cd, and Cs. On the contrary, TFF yielded a lower colloidal/nanoparticle proportion than DEF for Cu in upstream and downstream. Given that the particulate fractions or the colloidal/nanoparticle fractions only occupied a very small part (<10%) for most elements, the difference in these size fractions between two filtration modes were not so evident. In the case of TOC, the size fractions obtained by two filtration modes also showed the similar profiles, which indicates the partitioning of TOC was independent of filtration modes.

For these elements or TOC, as a conclusion, the influence of filtration modes on partitioning was not significant, when the membranes used and operational factors during filtration processes were the same.

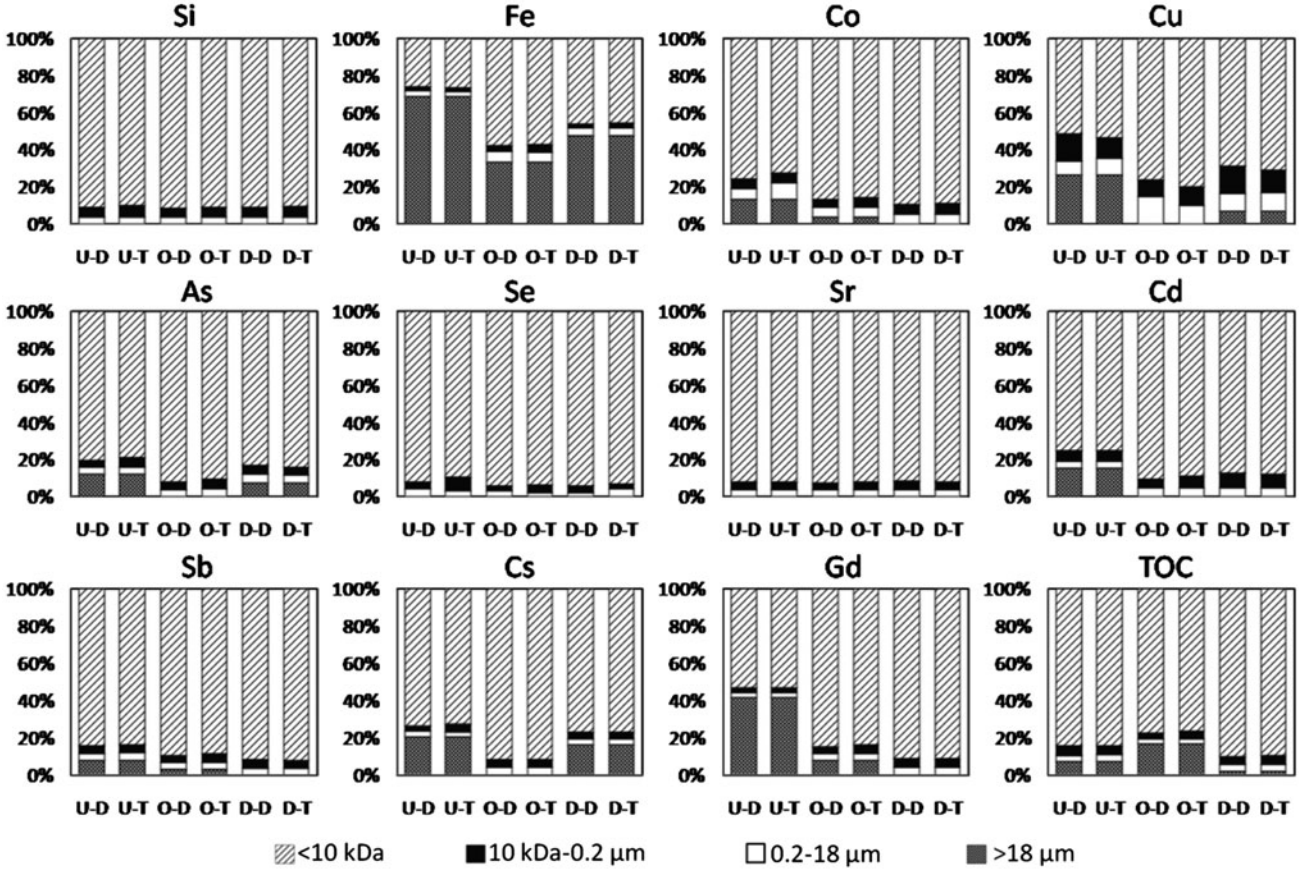

Fig. 6. Partitioning of elements for three sampling sites by two filtration modes (U-upstream; O-outlet; D before a dash: downstream; D after a dash: DEF; and T: TFF).

4. Conclusions

In this study, the impact of membrane filtration modes (DEF and TFF) on fractionation processes was studied. Surface water samples from upstream, WWTP effluent (outlet) of the IZ, and downstream of the Arc River were analyzed. For most elements, concentrations in different size fractions obtained by two filtration modes were generally similar. These results are supported by the validation of the mass balance. The obvious difference was only found in acid fractions for some elements, which might be related to the cake grown at membrane surfaces between two filtration modes. This observation is also in agreement with particle size analysis for 0.2 µm filtrations, which revealed that DEF resulted in particle aggregation to a larger degree than TFF, and this might be linked to the greater level of fouling during DEF. In case of elemental partitioning, the influence of filtration modes was normally negligible, when the membranes used and operational factors were exactly the same. Overall, the results obtained largely improved the understanding in filtration processes of aquatic elements.

Acknowledgements

This work has been carried out in the framework of the Labex MEC (ANR-10-LABX-0092) and of the AMIDEX project (ANR-11-IDEX-0001-02), funded by the « Investissements d'Avenir » French Government program managed by the French National Research Agency (ANR). We also acknowledge China Scholarship Council (CSC) for the scholarship.

References

[1] H.W. Chen, Gallium, indium, and arsenic pollution of groundwater from a semiconductor manufacturing area of Taiwan, Bull. Environ. Contam. Toxicol. 77 (2006) 289–296.
[2] S.C. Hsu, H.L. Hsieh, C.P. Chen, C.M. Tseng, S.C. Huang, C.H. Huang, Y.T. Huang, V. Radashevsky,

S.H. Lin, Tungsten and other heavy metal contamination in aquatic environments receiving wastewater from semiconductor manufacturing, J. Hazard. Mater. 189 (2011) 193–202.
[3] C. Neal, H. Jarvie, P. Rowland, A. Lawler, D. Sleep, P. Scholefield, Titanium in UK rural, agricultural and urban/industrial rivers: Geogenic and anthropogenic colloidal/sub-colloidal sources and the significance of within-river retention, Sci. Total Environ. 409 (2011) 1843–1853.
[4] M. Baalousha, J.R. Lead, Size fractionation and characterization of natural aquatic colloids and nanoparticles, Sci. Total Environ. 386 (2007) 93–102.
[5] N. Wu, Y. Wyart, Y. Liu, J. Rose, P. Moulin, An overview of solid/liquid separation methods and size fractionation techniques for engineered nanomaterials in aquatic environment, Environ. Technol. Rev. 2 (2013) 55–70.
[6] M.K. Pham, J.M. Garnier, Distribution of trace elements associated with dissolved compounds (<0.45 μm–1 nm) in freshwater using coupled (frontal cascade) ultrafiltration and chromatographic separations, Environ. Sci. Technol. 32 (1998) 440–449.
[7] M. Waeles, V. Tanguy, G. Lespes, R.D. Riso, Behaviour of colloidal trace metals (Cu, Pb and Cd) in estuarine waters: An approach using frontal ultrafiltration (UF) and stripping chronopotentiometric methods (SCP), Estuar. Coast. Shelf Sci. 80 (2008) 538–544.
[8] E.V. Vasyukova, O.S. Pokrovsky, J. Viers, P. Oliva, B. Dupré, F. Martin, F. Candaudap, Trace elements in organic- and iron-rich surficial fluids of the boreal zone: Assessing colloidal forms via dialysis and ultrafiltration, Geochim. Cosmochim. Ac. 74 (2010) 449–468.
[9] C. Guéguen, C. Belin, J. Dominik, Organic colloid separation in contrasting aquatic environments with tangential flow filtration, Water Res. 36 (2002) 1677–1684.
[10] J. Buffle, H.P. van Leeuwen, Environmental Particles, Environmental analytical an physical chemistry series (IUPAC), vol. 1, Lewis Publishers, Boca Raton, 1992.
[11] A. Wilding, R. Liu, J.L. Zhou, Dynamic behaviour of river colloidal and dissolved organic matter through cross-flow ultrafiltration system, J. Colloid Interface Sci. 287 (2005) 152–158.
[12] M. Hassellöv, K.O. Buesseler, S.M. Pike, M. Dai, Application of cross-flow ultrafiltration for the determination of colloidal abundances in suboxic ferrous-rich ground waters, Sci. Total Environ. 372 (2007) 636–644.
[13] F.J. Doucet, L. Maguire, J.R. Lead, Assessment of cross-flow filtration for the size fractionation of freshwater colloids and particles, Talanta 67 (2005) 144–154.
[14] N. Wu, Y. Wyart, J. Rose, B. Angeletti, P. Moulin, Size fractionation of elements in river water by both frontal filtration and tangential flow filtration, International Conference on Membranes (ICM-2013), October 3–6 (2013), Kottayam, India.
[15] EU drinking water standards, 1998. Available from: <http://www.lenntech.com/who-eu-water-standards.htm>. July 2014.
[16] C.L. Babiarz, S.R. Hoffmann, M.M. Shafer, J.P. Hurley, A.W. Andren, D.E. Armstrong, A critical evaluation of tangential-flow ultrafiltration for trace metal studies in freshwater systems. 2. Total mercury and methylmercury, Environ. Sci. Technol. 34 (2000) 3428–3434.
[17] M.A. Morrison, G. Benoit, Investigation of conventional membrane and tangential flow ultrafiltration artifacts and their application to the characterization of freshwater colloids, Environ. Sci. Technol. 38 (2004) 6817–6823.
[18] L.S. Wen, M.C. Stordal, D. Tang, G.A. Gill, P.H. Santschi, An ultraclean cross-flow ultrafiltration technique for the study of trace metal phase speciation in seawater, Mar. Chem. 55 (1996) 129–152.
[19] A. Dabrin, J.L. Roulier, M. Coquery, Colloidal and truly dissolved metal(oid) fractionation in sediment pore waters using tangential flow filtration, Appl. Geochem. 31 (2013) 25–34.
[20] B. Dupré, J. Viers, J.L. Dandurand, M. Polve, P. Bénézeth, P. Vervier, J.J. Braun, Major and trace elements associated with colloids in organic-rich river waters: Ultrafiltration of natural and spiked solutions, Chem. Geol. 160 (1999) 63–80.
[21] D. Perret, M.E. Newman, J.C. Nègre, Y. Chen, J. Buffle, Submicron particles in the rhine river—I. Physico-chemical characterization, Water Res. 28 (1994) 91–106.
[22] C. Casiot, M. Egal, F. Elbaz-Poulichet, O. Bruneel, C. Bancon-Montigny, M.A. Cordier, E. Gomez, C. Aliaume, Hydrological and geochemical control of metals and arsenic in a Mediterranean river contaminated by acid mine drainage (the Amous River, France); preliminary assessment of impacts on fish (*Leuciscus cephalus*), Appl. Geochem. 24 (2009) 787–799.
[23] L. Sigg, H. Xue, D. Kistler, R. Sshönenberger, Size fractionation (dissolved, colloidal and particulate) of trace metals in the Thur River, Switzerland, Aquat. Geochem. 6 (2000) 413–434.
[24] J.Y. Yu, M. Park, J. Kim, Solubilities of synthetic schwertmannite and ferrihydrite, Geochem. J. 36 (2002) 119–132.
[25] P. Aimar, M. Meireles, V. Sanchez, A contribution to the translation of retention curves into pore size distributions for sieving membranes, J. Membr. Sci. 54 (1990) 321–338.